Chinese Chemical Letters 31 (2020) 2087–2090

Contents lists available at ScienceDirect

Chinese Chemical Letters

journal homepage: www.elsevier.com/locate/cclet

Communication

Micro-spherical $ZnSnO_3$ material prepared by microwave-assisted method and its ethanol sensing properties

Dan Zhang, Yuqin Zhang, Yu Fan, Na Luo, Zhixuan Cheng*, Jiaqiang Xu*

NEST Lab, Department of Physics, Department of Chemistry, College of Science, Shanghai University, Shanghai 200444, China

ARTICLE INFO

Article history:
Received 27 November 2019
Received in revised form 25 December 2019
Accepted 2 January 2020
Available online 3 January 2020

Keywords:
$ZnSnO_3$ microspheres
Microwave synthesis
Morphology
Ethanol
Gas sensor

ABSTRACT

Monodispersed $ZnSnO_3$ microspheres are successfully prepared *via* a facile microwave-assisted method together with subsequently calcination treatment. Powder X-ray diffraction (PXRD) results indicate that the structure of the products shifted from crystalline to amorphous under high-temperature treatments. Field emission scanning electron microscope (FESEM) and the transmission electron microscope (TEM) observations demonstrate that the as-obtained products are composed of uniform microspheres with rough surfaces and the mean diameter is measured as ~700 nm. Moreover, the morphology of $ZnSnO_3$ microspheres can be well controlled by adjusting the ratio of Zn^{2+} and Sn^{4+}. The gas sensing properties of $ZnSnO_3$ microspheres with different ratios of Zn^{2+}/Sn^{4+} are investigated. Our results indicate that the $ZnSnO_3$ microspheres exhibit good selectivity and high sensitivity towards ethanol at the optimum working temperature of 230 °C. When the sensor is exposed 50 ppm ethanol, the value of response is 47 and the response/recovery times are 11 s and 12 s, respectively.

As a typical n-type semiconductor material, zinc stannate ($ZnSnO_3$) has a wide band-gap of 3.2 eV at room temperature [1]. $ZnSnO_3$ has been widely applied in many fields of bio/chemical sensing [2], photocatalysis [3], lithium ion battery [4,5] and energy storage [6] due to its merits such as good stability, low cost and non-toxic. It should be noted that $ZnSnO_3$ exhibits more potential applications in the field of gas sensors [7–9]. Particle size, morphology and structure of the gas sensing materials are the key factors to determine the performance of gas sensors. Various morphologies and structures of $ZnSnO_3$ can be obtained with different synthetic methods which make differences of gas sensing performance. During the past several decades, various morphologies of $ZnSnO_3$ were synthesized, such as nanoparticles [10,11], one-dimensional (1D) nanowires, nanorods, nanobelts [12–14], two-dimensional (2D) nanosheets, nanofilms [15] and three-dimensional (3D) nano-cubes, hollow microspheres, hollow nanocubes and hollow polyhedron [16,17]. In order to obtain different morphologies and structures of $ZnSnO_3$, many synthetic methods have been developed, including co-precipitation method, solid-phase synthesis, ion exchange method, hydrothermal method, thermal evaporation method and sol-gel method, *etc.* However, the above-mentioned synthetic methods have drawbacks in operation, high reaction temperature, long reaction time or high cost, which limit practical applications. Therefore, it is necessary to develop a facile and economical synthesis method to obtain $ZnSnO_3$.

Since 1980s, microwave-assisted method has been favored by more and more researchers in the field of chemistry [18–21]. Lu *et al.* [22] developed a simple calcination of $W_{18}O_{49}$ nanowires by a microwave-assisted solvothermal method to obtain flower-like WO_3 structures. The NO_2 and acetone sensing properties were investigated from flower-like WO_3. Sun *et al.* [23] reported that hierarchical Pd/SnO_2 nanostructures were prepared by a facile microwave-assisted method. The obtained material exhibits effective gas sensing performance to CO. Principle of microwave-assisted synthesis indicates that polar molecules can rearrange under electromagnetic field with the oscillation of the electric wave. In this process, electrical energy is converted into thermal energy due to friction and dielectric loss between the molecules. Compared with the conventional heating methods, microwave heating process exhibits higher reaction rate, shorter reaction time, lower energy consumption [24–27]. Therefore, the microwave synthesis technology becomes a green chemistry synthesis method, and is widely applied to prepare micro/nano materials.

In this paper, we developed a facile and environment-friendly microwave synthesis method to prepare $ZnSnO_3$ microspheres. Meanwhile, various morphologies of the $ZnSnO_3$ products can be obtained by adjusting the ratio of Zn^{2+}/Sn^{4+}. Furthermore, the gas

* Corresponding authors.
E-mail addresses: zxcheng@shu.edu.cn (Z. Cheng), xujiaqiang@shu.edu.cn (J. Xu).

https://doi.org/10.1016/j.cclet.2020.01.004

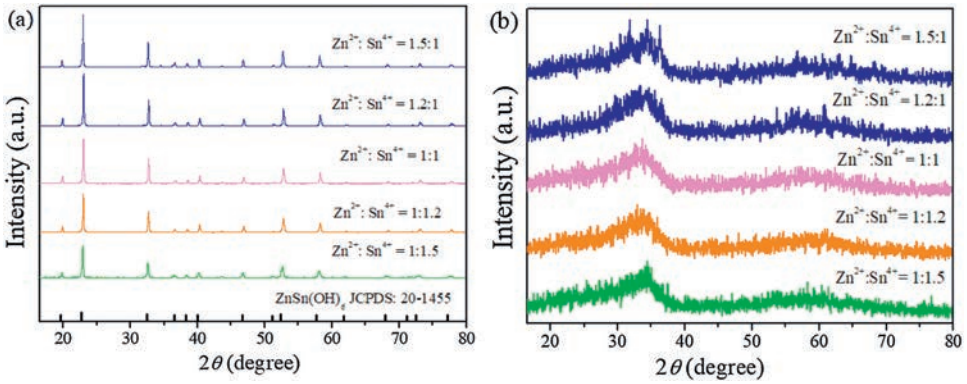

Fig. 1. (a) XRD patterns of $ZnSn(OH)_6$. (b) $ZnSnO_3$ products with different ratios of Zn^{2+} and Sn^{4+}.

sensing behaviors of $ZnSnO_3$ products with the different morphology were investigated. The results indicated that $ZnSnO_3$ microspheres exhibited ideal selectivity and high sensitivity to ethanol vapor.

PXRD patterns of $ZnSn(OH)_6$ and $ZnSnO_3$ products obtained with varied ratio of Zn^{2+}/Sn^{4+} are displayed in Fig. 1. As shown in Fig. 1a, all of the diffraction peaks are sharp and can be well matched to the standard card of $ZnSn(OH)_6$ (JCPDS No. 20-1455). No peaks are observed from impurities, suggesting that $ZnSn(OH)_6$ with high purity and good crystallization is obtained. After calcination at 400 °C, the products only have one wide diffraction peak as shown in Fig. 1b, which is similar result as mentioned in literature [28]. It is confirmed that $ZnSnO_3$ with amorphous structure can be obtained after calcinating $ZnSn(OH)_6$.

The morphologies of $ZnSn(OH)_6$ and $ZnSnO_3$ microspheres with the ratio 1:1 of Zn^{2+}/Sn^{4+} are characterized by SEM, and (HR)-TEM in Fig. 2. Obviously, in Fig. 2a, $ZnSn(OH)_6$ microspheres with the size distribution between 600–800 nm is self-assembled with some nanoparticles. After calcination of $ZnSn(OH)_6$ microspheres, spherical shape $ZnSnO_3$ with well-dispersed are formed as clear from SEM and TEM images in Figs. 2b and c. The diameter of the $ZnSnO_3$ product is measured as ~700 nm and the surface of the microspheres is rough. Compared with the $ZnSn(OH)_6$, surface roughness of $ZnSnO_3$ microspheres is increased due to the loss of crystal water during calcination process. There is no lattice fringe of $ZnSnO_3$ microspheres seen in (HR)-TEM image (Fig. 2d) so it is amorphous structure. The HRTEM result is consistent with the XRD data as shown in Fig. 1b.

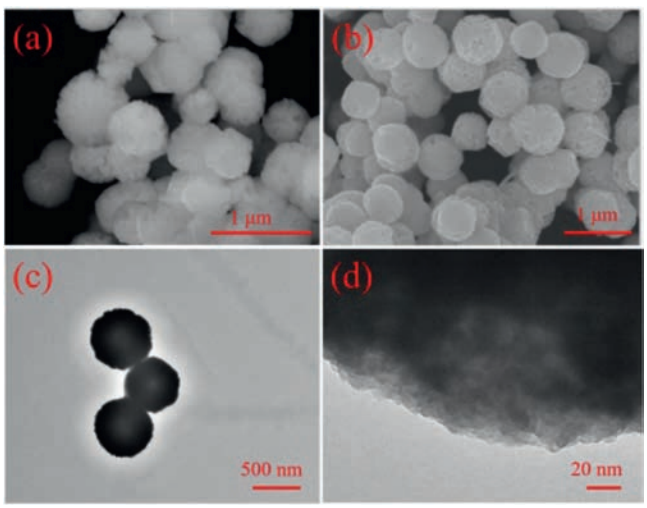

Fig. 2. SEM images of (a) $ZnSn(OH)_6$ and (b) $ZnSnO_3$ microspheres. (c) TEM and (d) HRTEM images of the $ZnSnO_3$ microspheres.

The effect of Zn^{2+}/Sn^{4+} ratio on microstructure of $ZnSnO_3$ products is further investigated by SEM. Fig. 3 shows the SEM images of $ZnSnO_3$ products obtained with different ratios of Zn^{2+}/Sn^{4+}. When the ratio of Zn^{2+}/Sn^{4+} is 1:1.5, abundant cubes and a few truncated octahedrons were observed in the $ZnSnO_3$ products, and the particles size are between 500 nm and 1000 nm (Fig. 3a). When the ratio of Zn^{2+}/Sn^{4+} is 1:1.2, $ZnSnO_3$ product features irregular micro-spherical morphology with a wide diameter range of 500–900 nm (Fig. 3b). When the ratio of Zn^{2+}/Sn^{4+} is 1.2:1, $ZnSnO_3$ product has a mass of truncated octahedrons with the diameter of 1200–1800 nm (Fig. 3c). When the ratio of Zn^{2+}/Sn^{4+} is 1.5:1, $ZnSnO_3$ product is consisted of truncated polyhedrons with the diameter of 1400–1900 nm (Fig. 3d).

The above-mentioned experimental results indicate that the morphology of $ZnSnO_3$ products changes from polyhedrons to microspheres to polyhedrons along with the Zn^{2+}/Sn^{4+} ratio increases. Therefore, it can deduce that the atomic arrangement in the crystal cells of $ZnSn(OH)_6$ is related to Zn^{2+}/Sn^{4+} ratio (Fig. 4). With the increased Zn^{2+}/Sn^{4+} ratio, excessive Zn atoms will replace and occupy the position of Sn atoms (Fig. 4a), in contrast, excessive Sn atoms will replace and occupy the position of Zn atoms (Fig. 4c), which bringing different surface energies in the same crystal plane. As a result the $ZnSnO_3$ products present different polyhedral morphologies including cube and polyhedron, which may be contributed by the different growth kinetics in the crystal planes of $ZnSn(OH)_6$ with various Zn^{2+}/Sn^{4+} ratios.

After that, the $ZnSnO_3$ products are used as sensing material to fabricate gas sensors and its sensing properties are inspected. Firstly, important parameters of working temperature and selectivity are investigated. In order to obtain the optimum working temperature, the response of the sensors based on $ZnSnO_3$ materials to 50 ppm ethanol are tested and shown in Fig. 5a. It can be seen that the responses of the sensors increase when temperature rises and the response reaches a maximum value at 230 °C. Therefore, 230 °C is selected as the optimum working temperature for further exploring gas sensing properties of the as-prepared materials. Fig. 5b shows the sensing responses of $ZnSnO_3$-based sensors towards eight kinds of gases including C_2H_5OH, CH_3OH, HCHO, CH_3COCH_3, C_6H_6, C_7H_8, CO and $CHCl_3$ (all with concentration of 50 ppm). Obviously, the $ZnSnO_3$ sensors exhibit a satisfactory selectivity to ethanol compared to the other gases. Also, the sensor based on $ZnSnO_3$ material with Zn^{2+}/Sn^{4+} ratio of 1:1 shows the maximum response of 47 to ethanol. Thus, $ZnSnO_3$ material with Zn^{2+}/Sn^{4+} ratio of 1:1 is optimized for ethanol detection in the following measurements.

Fig. 5c shows the sensing curve of the micro-spherical $ZnSnO_3$ microspheres sensor to ethanol with concentration ranging from 1

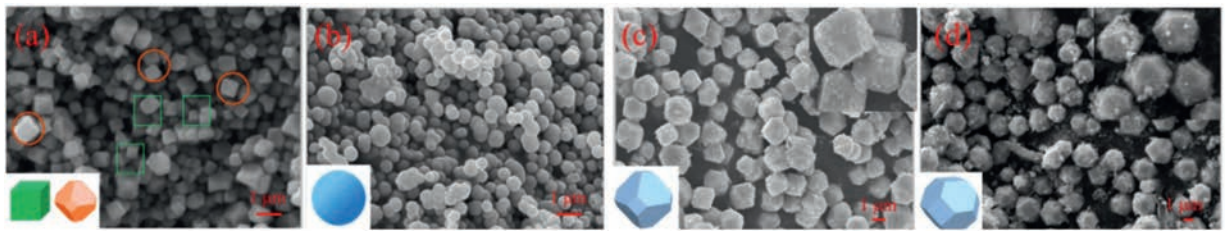

Fig. 3. SEM images of the $ZnSnO_3$ products with the varied ratio of the Zn^{2+} and Sn^{4+}: (a) Zn^{2+}/Sn^{4+} = 1:1.5; (b) Zn^{2+}/Sn^{4+} = 1:1.2; (c) Zn^{2+}/Sn^{4+} = 1.2:1; (d) Zn^{2+}/Sn^{4+} = 1.5:1. The insets of (c) and (d) show the high resolution SEM images of the corresponding material.

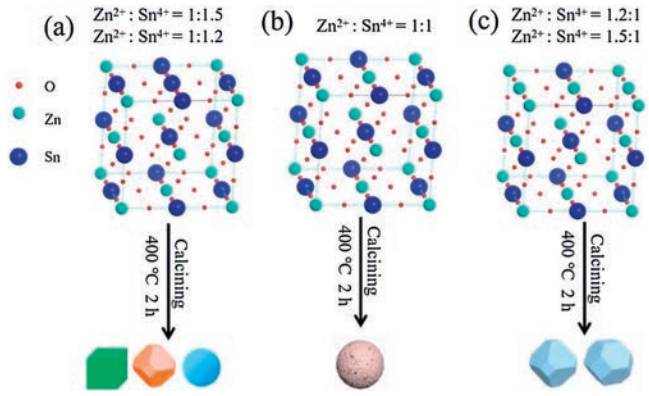

Fig. 4. Formation mechanism of $ZnSnO_3$ products: (a) Zn^{2+}/Sn^{4+} = 1:1.5, Zn^{2+}/Sn^{4+} = 1:1.2; (b) Zn^{2+}/Sn^{4+} = 1:1; (c) Zn^{2+}/Sn^{4+} = 1.2:1, Zn^{2+}/Sn^{4+} = 1.5:1.

to 200 ppm at 230 °C. When the sensor exposed to ethanol vapor, the sensor immediately outputs a voltage sensing signal. After detection, the voltage signal can be almost back to its initial value when the testing atmosphere is switched to fresh air. Our measurements also indicate that the sensor has a high sensitivity to ethanol. In Fig. 5d, the detection of limit (LOD) is better than 1 ppm since the response value is measured as 3 at the ethanol concentration of 1 ppm. It is worth noting that below 10 ppm there is a linear relation between the response values and ethanol concentrations. Fig. 5e shows the one-cycle testing curve of the sensor based on $ZnSnO_3$ microspheres to 50 ppm ethanol at 230 °C, which indicates that the sensor has a fast response/recovery performance to ethanol and the respond and recover time is measured as 11 s and 12 s, respectively. In addition, the sensing response is tested continuously for more than three months to evaluate the long-term stability of the sensor based on $ZnSnO_3$ microspheres. The data in Fig. 5f indicate that there is only a slightly decrease of the sensing response after 120 days, which indicates good stability of the sensor.

As an n-type semiconductor material, $ZnSnO_3$ has a high concentration of charge carriers and abundant active centers existing on its surface. When the sensor is exposed to air, oxygen molecules are adsorbed on the surface of the $ZnSnO_3$ microspheres and capture electrons from the conduction band of the sensitive material to form oxygen species such as O_2^- or O^- [29,30]. Therefore, an electron depletion layer (with thickness of d) is formed with the high resistance state of $ZnSnO_3$ microspheres. Some typical reactions are shown as follows.

$$O_2\ (gas) \leftrightarrow O_2\ (ads) \quad (1)$$

$$O_2\ (ads) + e^- \leftrightarrow O_2^-\ (ads) \quad (2)$$

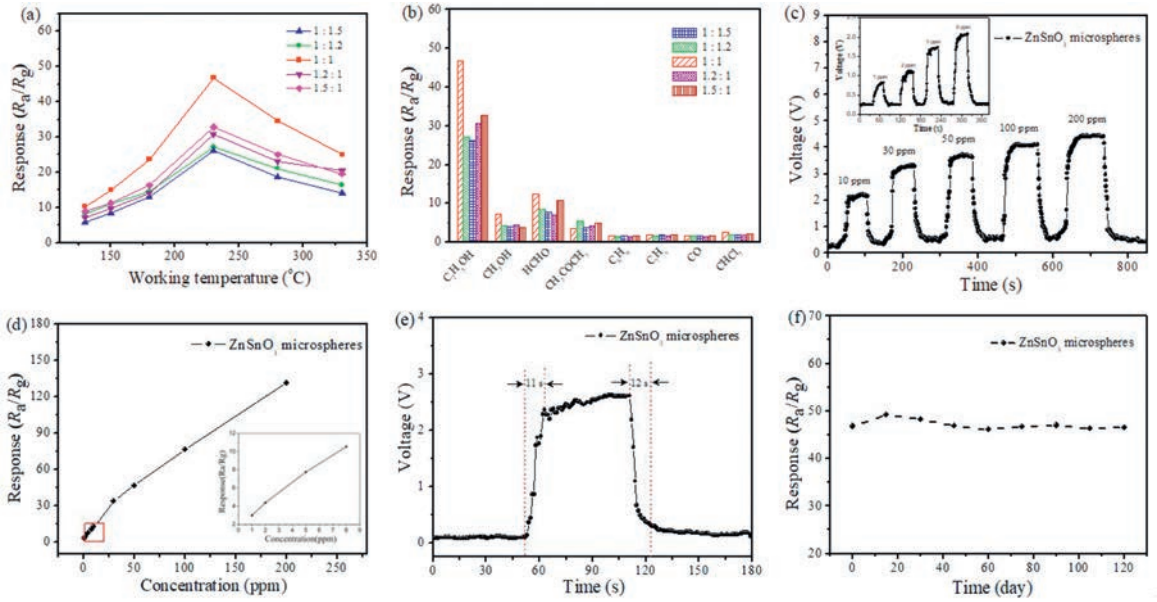

Fig. 5. Gas-sensing properties of the $ZnSnO_3$ products. (a) Sensors based on $ZnSnO_3$ products toward 50 ppm ethanol at different temperature. (b) Gas response toward 50 ppm various gases at 230 °C. (c) Dynamic response-recovery curve of the sensor based on $ZnSnO_3$ microspheres to 1–200 ppm ethanol; inset is 1–8 ppm ethanol. (d) Rhe relationship of gas response and concentration. (e) Response-recovery curve to 50 ppm ethanol. (f) The long-term stability of the sensor based on $ZnSnO_3$ microspheres.

$$O_2^- (ads) + e^- \leftrightarrow 2O^- (ads) \quad (3)$$

$$O^- (ads) + e^- \leftrightarrow O^{2-} (ads) \quad (4)$$

The chemisorbed oxygen species is mainly O^- at the optimum working temperature of 230 °C. When the sensor is exposed to ethanol vapor, the chemisorbed oxygen species react with ethanol molecules and release the electrons back to the materials. The abovementioned reaction decreases the thickness *d* of the electron depletion layer and a low resistance state is formed. The related reaction is explained as follows.

$$C_2H_5OH (g) + 6O^- (ads) \rightarrow 2CO_2 + 3H_2O + 6e^- \quad (5)$$

Compared with the other $ZnSnO_3$ products (Figs. 3b–d) in this work, the prepared $ZnSnO_3$ microspheres feature uniform particle size with less agglomeration. In the basis of our speculation, the contact surface of the microspheres has a small grain boundary resistance, which is facilitates to electron transport and leads to enhance the gas sensing performance including sensitivity and selectivity. Thus, $ZnSnO_3$ microspheres material is a good candidate for ethanol detection.

In summary, monodisperse $ZnSnO_3$ microspheres with the diameters of ~700 nm are prepared by a facile and green synthesis route using microwave-assisted method. Meanwhile, $ZnSnO_3$ products with various particle size and controllable morphology are synthesized by adjusting the ratio of Zn^{2+} and Sn^{4+}. Compared with the other shapes of $ZnSnO_3$ microstructures, $ZnSnO_3$ microspheres exhibit superior gas-sensing properties towards ethanol vapors. The measurement results reveal that the response value of the sensor reaches 47–50 ppm ethanol vapor at 230 °C and the response/recovery times are 11 s and 12 s, respectively. The high sensitivity, good selectivity, short response/recovery times and satisfactory stability of the prepared sensor suggest that the micro-spherical $ZnSnO_3$ material in this study is a reliable candidate for ethanol detection.

Declaration of competing interest

The authors declare that they have no known competing financial interests or personal relationships that could have appeared to influence the work reported in this paper.

Acknowledgments

This research was supported by National Nature Science Foundation of China (Nos. 61671284 and U1704255). The authors are grateful to the help of Instrumental Analysis and Research Center in Shanghai University for material characterization.

Appendix A. Supplementary data

Supplementary material related to this article can be found, in the online version, at doi:https://doi.org/10.1016/j.cclet.2020.01.004.

References

[1] X. Wang, Y. Liu, B. Ding, et al., Sens. Actuator. B –Chem. 276 (2018) 211–221.
[2] J. Sun, S. Bai, Y. Tian, et al., Sens. Actuator. B –Chem. 257 (2018) 29–36.
[3] C. Liu, A. Piyadasa, M. Piech, et al., J. Mater. Chem. C 4 (2016) 6176–6184.
[4] F. Han, W.C. Li, C. Lei, B. He, K. Oshida, A.H. Lu, Small 10 (2014) 2637–2644.
[5] Y. Wang, D. Li, Y. Liu, J. Zhang, Mater. Lett. 167 (2016) 222–225.
[6] R. Guo, Y. Guo, H. Duan, H. Li, H. Liu, ACS Appl. Mater. Interfaces 9 (2017) 8271–8279.
[7] X. Jia, M. Tian, R. Dai, et al., Sens. Actuator. B –Chem. 240 (2017) 376–385.
[8] T. Zhou, T. Zhang, R. Zhang, et al., ACS Appl. Mater. Interfaces 9 (2017) 14525–14533.
[9] M. Xia, H. Li, M. Li, et al., Sens. Actuator. B –Chem. 264 (2018) 119–127.
[10] J. Li, T. Fu, Y. Chen, et al., Cryst. Eng. Comm. 16 (2014) 2977–2983.
[11] M. Miyauchi, Z. Liu, Z.G. Zhao, S. Anandan, K. Hara, Chem. Commun. 46 (2010) 1529–1531.
[12] A. Datta, D. Mukherjee, C. Kons, et al., Small 10 (2014) 4093–4099.
[13] X. Jia, C. Cheng, S. Feng, et al., Appl. Surf. Sci. 481 (2019) 1001–1010.
[14] J.M. Wu, C. Xu, Y. Zhang, et al., Adv. Mater. 24 (2012) 6094–6099.
[15] S. Singh, A. Singh, M. Wan, et al., Sens. Actuator. B –Chem. 205 (2014) 102–110.
[16] K.Y. Lee, D. Kim, J.H. Lee, et al., Adv. Funct. Mater. 24 (2014) 6948.
[17] X. Jia, C. Cheng, S. Yu, et al., Sens. Actuator. B –Chem. 300 (2019)127012.
[18] Y.C. Ko, C.F. Tsai, C.C. Wang, et al., J. Am. Chem. Soc. 136 (2014) 14425–14431.
[19] J. Fan, B.M. De, V.L. Budarin, et al., J. Am. Chem. Soc. 135 (2013) 11728–11731.
[20] X. Du, T. Yang, J. Lin, et al., ACS Appl. Mater. Interfaces 8 (2016) 15598–15606.
[21] N. Garino, A. Sacco, M. Castellino, et al., ACS Appl. Mater. Interfaces 8 (2016) 4633–4643.
[22] Z. Wang, P. Sun, T. Yang, et al., Sens. Actuator. B –Chem. 186 (2013) 734–740.
[23] Q. Wang, C. Wang, H. Sun, P. Sun, G. Lu, Sens. Actuator. B –Chem. 222 (2015) 257–263.
[24] H. Song, S. Yan, Y. Yao, et al., Chem. Eng. J. 370 (2019) 1331–1340.
[25] H.J. Kitchen, S.R. Vallance, J.L. Kennedy, et al., Chem. Rev. 114 (2014) 1170–1206.
[26] S. Nekkanti, K. Veeramani, K.N. Praveen, et al., Green Chem. 18 (2016) 3439–3447.
[27] R. Sood, A. Donnadio, S. Giancola, et al., ACS Appl. Mater. Interfaces 8 (2016) 16897–16906.
[28] X. Jia, M. Tian, R. Dai, et al., Sens. Actuator. B –Chem. 240 (2016) 376–385.
[29] Y. Li, D.L. Li, J.C. Liu, Chin. Chem. Lett. 26 (2015) 304–308.
[30] P. Song, Q. Wang, Z. Yang, Sens. Actuator. B –Chem. 156 (2011) 983–989.